Different Propensity to Form Amyloid Fibrils by Two Homologous Proteins—Human Stefins A and B: Searching for an Explanation

Saša Jenko,[1] Miha Škarabot,[2] Manca Kenig,[1] Gregor Gunčar,[1] Igor Muševič,[2] Dušan Turk,[1] and Eva Žerovnik[1]*
[1]*Department of Biochemistry and Molecular Biology, Jožef Stefan Institute, Ljubljana, Slovenia*
[2]*Department of Condensed Matter Physics, Jožef Stefan Institute, Ljubljana, Slovenia*

ABSTRACT **By using ThT fluorescence, X-ray diffraction, and atomic force microscopy (AFM), it has been shown that human stefins A and B (subfamily A of cystatins) form amyloid fibrils. Both protein fibrils show the 4.7 Å and 10 Å reflections characteristic for cross β-structure. Similar height of ~3 nm and longitudinal repeat of 25–27 nm were observed by AFM for both protein fibrils. Fibrils with a double height of 5.6 nm were only observed with stefin A. The fibril's width for stefin A fibrils, as observed by transmission electron microsopy (TEM), was in the same range as previously reported for stefin B (Žerovnik et al., Biochem Biophys Acta 2002;1594:1–5). The conditions needed to undergo fibrillation differ, though. The amyloid fibrils start to form at pH 5 for stefin B, whereas in stefin A, preheated sample has to be acidified to pH < 2.5. In both cases, adding TFE, seeding, and alignment in a strong magnetic field accelerate the fibril growth. Visual analysis of the three-dimensional structures of monomers and domain-swapped dimers suggests that major differences in stability of both homologues stem from arrangement of specific salt bridges, which fix α-helix (and the α-loop) to β-sheet in stefin A monomeric and dimeric forms. Proteins 2004;55:417–425.**

Key words: cystatin; amyloid fibril; domain-swapped dimer; ionic interactions; conformational disease; AFM; X-ray diffraction; protein modeling

INTRODUCTION

Amyloidoses are various systemic and localized diseases with a common feature of "amyloid". Amyloid plaques are composed from deposits of misfolded proteins and some other nonproteinaceous components, such as serum amyloid P, heparan sulfate proteoglycans, and apolipoprotein E.[1,2] Because changed protein conformation (misfolding) leads to protein aggregation and deposition, amyloidoses are also called conformational diseases. Among them are neurodegenerative and prion diseases with extracellular or intracellular inclusions.[3–5]

A common low-resolution structure has been observed to date for most of the amyloid fibrils. Amyloid fibrils share a common molecular skeleton, the protofilament core structure, which is a continuous β-sheet helix.[6–9] The reflections at ~4.7 Å on the meridian and 10 Å on the equator are seen in all amyloid fiber diffraction patterns. The structural repeat of 4.7 Å along the fiber axis corresponds to the spacing of β-strands, and the 10–12 Å spacing corresponds to the face to face separation of the β-sheets.[10]

Atomic force microscopy (AFM) has become a very important tool for the observation of surface morphology of amyloid fibrils[11–14] and the kinetics of their growth.[15] When fibrils are deposited to the flat solid surface, it is possible to obtain accurate measurements of the height and the length of fibrils, whereas the width is overestimated because of the finite size of the tip. The periodicity of the height along the fibril can also determined.

Human stefins are structurally well-characterized proteins. By the new nomenclature MEROPS, 6.1 release http://merops.sanger.ac.uk/, they are classified as subfamily A of the family I25 of cystatins. Three-dimensional (3D) structure of stefin B in complex with papain[16] and that of stefin A in complex with cathepsin H[17] have been determined. Solution structure of stefin A has also been determined by heteronuclear NMR.[18] It has been shown that stefin A forms a dimer at predenaturational temperatures,[19] which is divided from the monomer by a high energetic barrier.[19] The solution structure of the domain-swapped dimer has been revealed by NMR,[20] and a crystallographic structure was determined for cystatin C domain-swapped-dimer.[21]

Stability and folding studies of the two homologous proteins have revealed major differences.[22,23] In stefin B, intermediates in GuHCl and acid denaturation have been observed,[24,25] whereas stefin A behaved two-state.[26] Stability against TFE solvent was compared,[23] the titration ending with an all α-helical denatured state, in both stefins. An α-helical folding intermediate[27] was detected in stefin B folding only.[22,23]

Grant sponsor: Slovenian Ministry of Education, Science, and Sport.

*Correspondence to: Eva Žerovnik, Department of Biochemistry and Molecular Biology, Jožef Stefan Institute, Jamova 39, 1000, Ljubljana, Slovenia. E-mail: eva.zerovnik@ijs.si

Received 24 July 2003; Accepted 29 October 2003

Published online 5 March 2004 in Wiley InterScience (www.interscience.wiley.com). DOI: 10.1002/prot.20041

Recently, it was shown that the recombinant human stefin B forms amyloid fibrils rather easily, in contrast to its homologue, recombinant human stefin A.[28–31] Under properly chosen conditions,[31] this protein, as probably proteins in general,[32] does transform into amyloid fibrils. It is of interest that amyloidogenic proteins (or their fragments) not involved in any known disease are toxic for the cells,[33] implying a generic mechanism for toxicity as well.

In this article we demonstrate that amyloid fibrils of both stefins, proteins of 53% identity, share common structural features characteristic for other amyloid fibrils. To illustrate the structure of the amyloid fibrils, three techniques were used: ThT fluorescence, X-ray diffraction, and AFM. We also describe the influence of seeding and magnetic field on the rate of fibrillation. Finally, 3D structures and models of monomeric and dimeric states have been analyzed to find any difference between the two homologues, which may help to explain their different propensities to form amyloid fibrils.

MATERIALS AND METHODS

Chemicals

All chemicals were at least of analytical grade. 2,2,2 Trifluoroethanol (TFE) was from Fluka (Buchs, Switzerland), 99% pure. Thioflavine T (ThT) was from Aldrich, (Milwaukee, WI). Solvents were prepared with double-distilled water and filtered through 0.22-μm filters.

Preparations of Stefins A and B

Recombinant human stefins A and B were prepared as described.[34,35]

Stefin A and B Fibril Formation

Stefin A fibril formation was induced by dissolving a preheated sample (2 h at 86°C) at pH 2.5 (0.015 M glycine buffer, pH 2.48, 0.15 M NaCl, protein concentration c_i = 100 μM). Fibril formation was accelerated by adding 30 μL of previously formed stefin A fibrils as a seed to one half of the sample ($V_{s1/2}$ = 1 mL). Fibril growth was followed in four samples of stefin A (2 controls: stefin A alone, stefin A with the fibril seed and 2 samples in a 2T magnetic field: stefin A alone, stefin A with the fibril seed).

Stefin B fibrils were grown under mild conditions at pH slightly below 5 (0.015 M acetate buffer, 0.15 M NaCl, pH = 4.77, protein concentration c_i = 44 μM). Fibril formation was accelerated by adding 30 μL of previously formed stefin B fibrils as a seed to one third of the sample ($V_{s1/3}$ = 1 mL) and adding 10% TFE to another one third of the sample. Therefore, fibril growth was followed in six samples of stefin B (3 controls: stefin B alone, stefin B with the fibril seed, and stefinB with 10% TFE, and 3 samples in a 2T magnetic field: stefin B alone, stefin B with the fibril seed, and stefin B with 10% TFE).

ThT Fluorescence Measurements

The Perkin Elmer model LS 50 B luminescence spectrometer was used for measuring the fluorescence spectra. Excitation was at 440 nm and spectra were recorded from 455 to 580 nm. Excitation and emission slits were set at 5 mm and 7 mm, respectively. Five microliters of the protein solution in which fibrils were growing were dissolved in 600 μL of the ThT buffer (pH 7.5, 25 mM phosphate buffer, 20 μM ThT) just before the measurement.

X-Ray Diffraction

Amyloid fibrils formed by stefins A and B were taken out of the 2.3 T magnet of a Brucker Biospec System, centrifuged, and dialyzed against distilled water. The fibrils were then placed in a glass capillary 1 day before measurement. Diffraction pattern was taken at in-house source using Cu Kα radiation from a Rigaku rotating anode X-ray generator RU200 and recorded on a 345-mm MAR Research image plate detector.

Atomic Force Microscopy

Ten microliters of stefin A or stefin B sample (around 45-μM protein concentration) were spread across freshly cleaved mica surface (1 cm^2), incubated for 5 min and gently washed with pH 4.7 solvent and deionized water. Excess water was removed with a stream of nitrogen. Images were obtained with a Nanoscope III Multimode scanning probe microscope (Digital Instruments) operating in contact and tapping mode. Because both methods gave the same results; we present images in contact mode only, where the resolution was better. Oxide-sharpened Si_3-N_4 tips with a nominal spring constant of 0.05 N/m and typical radiuses of 15 nm from Park Scientific Instruments were used. AFM images were obtained in the contact mode under $<$0.1 nN probe force at a pixel number of 512 $\times$ 512 and at a scan rate of 5 Hz.

3D Structure Analysis

3D structures of stefins (Fig. 1) were analyzed by using deposited coordinates from PDB for the monomer of stefin B,[16] for the monomer of stefin A,[17] and for the domain-swapped dimer of stefin A.[20] The domain-swapped dimer of stefin B was modeled by using MAIN program[36] with stefin A domain-swapped dimer[20] as a template.

RESULTS

ThT Fluorescence Derived Kinetics of Amyloid Fibril Formation

ThT fluorescence can be considered a complementary method for amyloid fibril quantitation. Thioflavine T undergoes characteristic spectral alterations on binding to a variety of amyloid fibrils.[37] Measurements of ThT fluorescence must be made in $<$1 min after dilution of the sample into the high pH solution that optimizes the ThT signal because at the same time high pH causes depolymerization of the fibrils.[37] In both stefins, the highest ThT fluorescence intensity is observed at pH 7.5 and not at 8.5; therefore, a buffer of pH 7.5 was used. The formation of amyloid fibrils was measured by taking 5-μL aliquots of a reaction mixture incubated under appropriate conditions and reading the fluorescence after dilution into 600 μL of ThT-containing buffer.

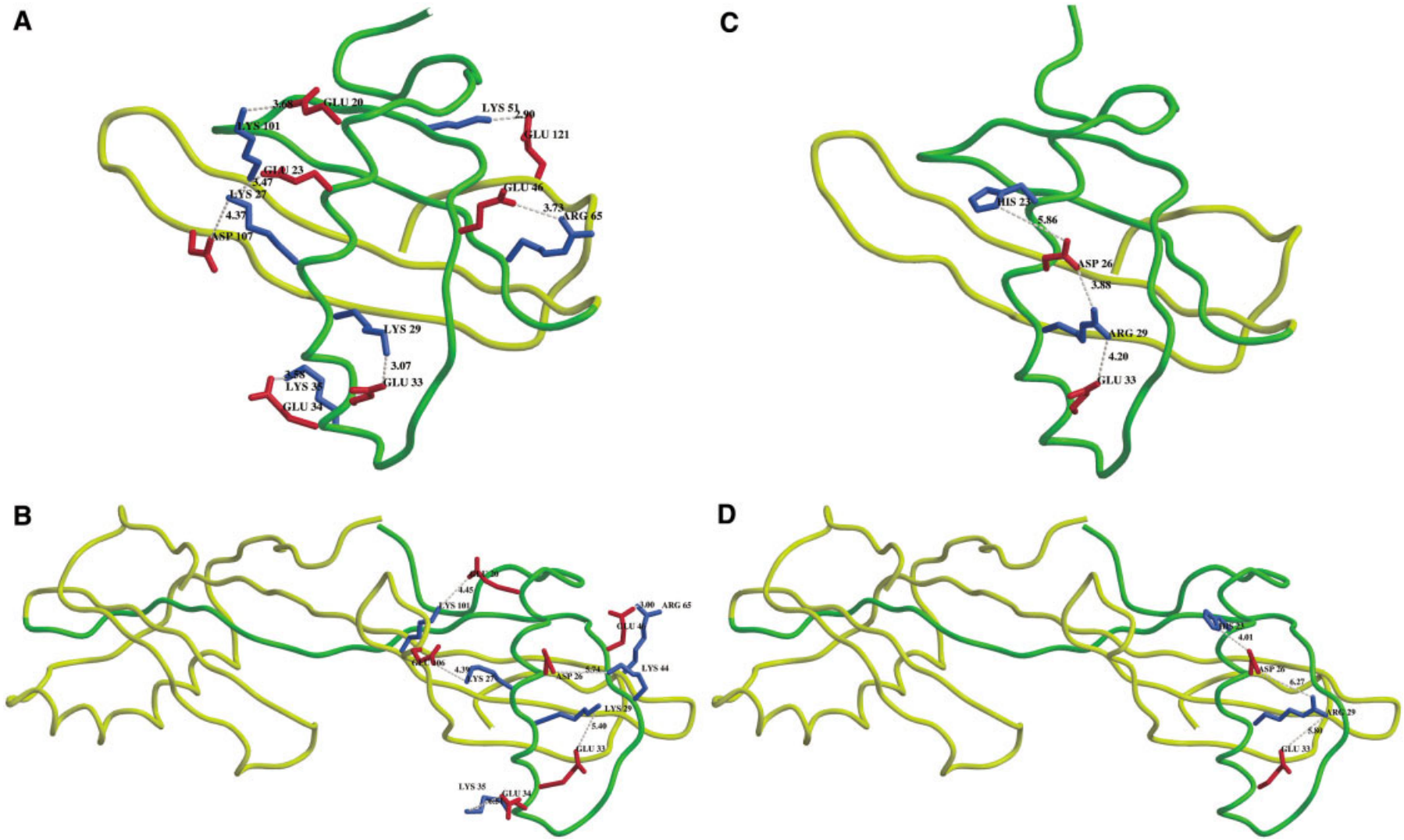

Fig. 1. **A:** The interchangeable tandem of α-helix and strand 2 of stefin A monomer in green[17] are attached via three salt bridges (Glu20-Lys101, Lys27-Asp107, and Lys51-Glu121) to the β-surface (strands 3–5) in green. α-Helix is internally stabilized by three salt bridges (Glu23-Lys27, Lys29-Glu33, and Glu34-Lys35), and strand 2 is attached by Glu46-Arg65 salt bridge to strand 1. The figure was prepared with the program MAIN.[36] The image file was rendered with the Raster3D program.[50] **B:** Ribbon plot of the stefin A swapped-dimer with the interchangeable region in green. α-Helix is attached via two salt bridges to the β-surface [Glu20 (15)-Lys101(71), Lys101(71)-Glu106(78)], and position of strand 2 is stabilized with the Glu46(39)-Arg65(58) and Asp26(21)-Lys44(37) salt bridges. Two internal salt bridges of α-helix are indicated [Lys29 (24)-Glu33 (28), Glu34 (29)-Lys35 (30)]. The dimer is numbered according to residues topologically equivalent in stefin A monomer,[17] with stefin A swapped-dimer[20] numbering in brackets. The image file was prepared with the program MAIN[36] and rendered with the Raster3D program.[50] **C:** α-Helix of stefin B monomer[16] is internally stabilized with three salt bridges (His23-Asp26, Asp26-Arg29, and Arg29-Glu33). The figure was prepared with the program MAIN.[36] The image file was rendered with the Raster3D program.[50] **D:** Ribbon plot of the model of stefin B swapped-dimer with the interchangeable region in green. Three internal salt bridges of α-helix are indicated (His23-Asp26, Asp26-Arg29, and Arg29-Glu33). The model was created by superposition on the stefin A swapped-dimer structure[20] with the program MAIN.[36] The dimer is numbered according to residues topologically equivalent in stefin B monomer. The image file was rendered with the Raster3D program.[50]

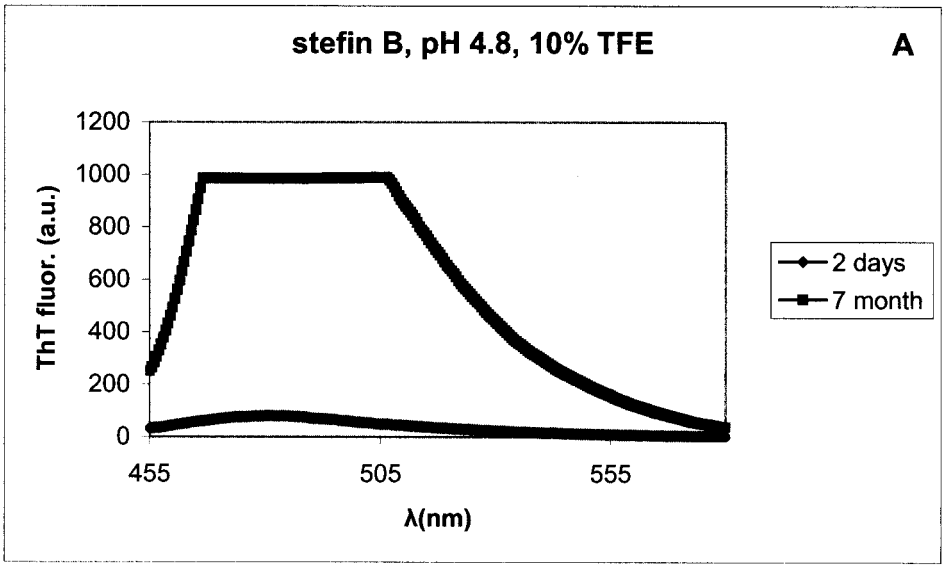

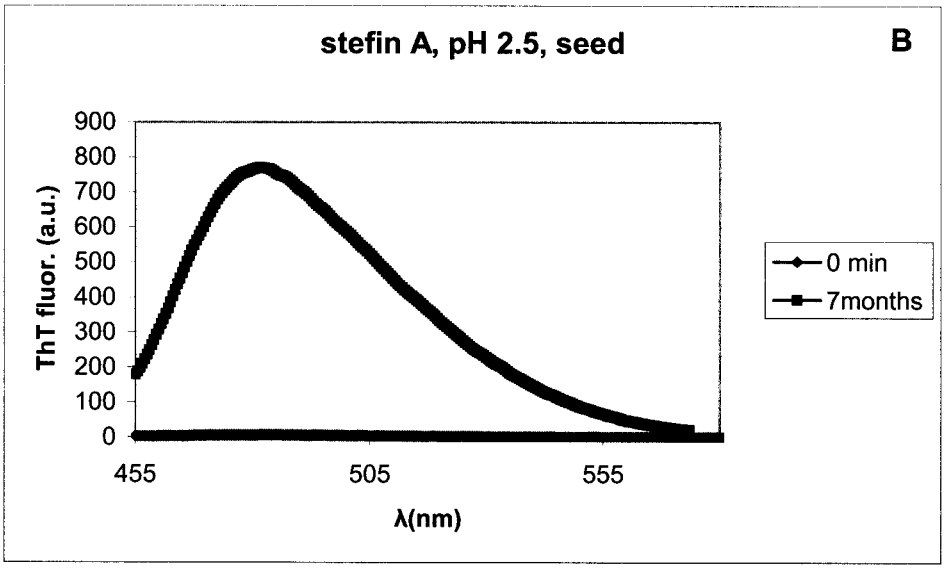

Fig. 2. Fluorescence emission spectra of Thioflavin T (ThT) dye in the presence of stefin B in arbitrary units (a.u.). Excitation was at 440 nm and spectra were recorded from 455 to 580 nm. **A:** Stefin B fibrils after 7 months of growth. Fibrils were grown in the magnet in the pH 4.8 buffer with 10% TFE. This is the same sample as for X-ray diffraction. **B:** Stefin A fibrils after 7 months at pH 2.5 with added seed. The same sample was observed by X-ray diffraction.

In Figure 2(A), the initial and final ThT fluorescence spectra of the stefin B sample taken for X-ray diffraction are shown. In Figure 2(B), the initial and final ThT fluorescence spectra of the stefin A sample taken for X-ray diffraction are shown. For all the prepared samples (described in Materials and Methods), the time course of fibrillation was followed (i.e., intensity of the fluorescence emission at 480 nm was plotted against time). In Figure 3(A) and (B), the kinetics of fibril growth for stefin B with added seed [Fig. 3(A)] and with 10 (v/v) % TFE [Fig. 3(B)] are shown as an example. Two samples were compared in each case: one grown in the magnet (filled triangles) and the other grown outside the magnet (filled diamonds). All the reactions were observed at room temperature, which was ~25°C.

Orientation of the Fibrils and Acceleration of Their Growth

We have put aqueous solutions of the amyloid fibrils in a 2.3-T magnetic field to facilitate alignment of the fibrils during their formation and let them grow for 4 months, constantly monitoring the fibril formation with ThT fluo-

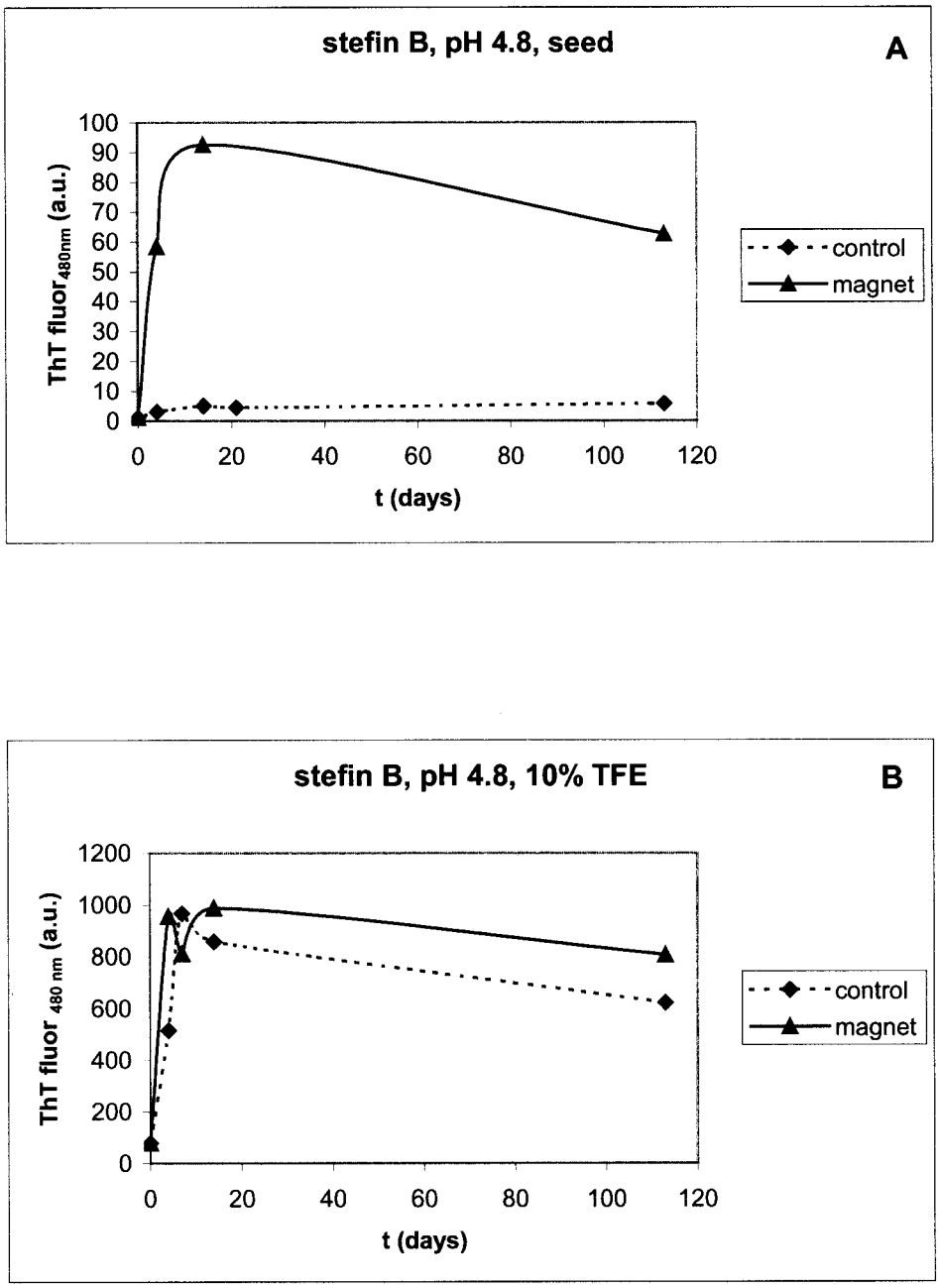

Fig. 3. ThT fluorescence emission intensity in arbitrary units (a.u.) plotted against time. (▲) sample in the magnet (♦) sample outside the magnet **A:** ThT fluorescence intensity at 480 nm of a stefin B sample grown at pH 4.8, seeded with sonificated preformed fibrils, diluted in ThT buffer (pH 7.5) at different times of fibril growth. **B:** ThT fluorescence intensity at 480 nm of a stefin B sample grown at pH 4.8 with 10% TFE, diluted in ThT buffer (pH 7.5) as a function of time of the fibril growth.

rescence measurements. We observed accelerated fibril growth in both cases where the seed was added: 3-fold for stefin A and 50-fold for stefin B [Fig. 3(A)]. No effect of the magnetic field was observed with stefins A and B dissolved in pure buffers (no seed or TFE added). In stefin B with TFE [Fig. 3(B)], the effect of the magnetic field may be surplused by the effect of TFE.

X-Ray Fiber Diffraction of Amyloid Fibrils

Fibril diffraction data indicate two powder-like concentric rings at ~4.7Å and ~10Å, corresponding to the interstrand hydrogen bond distance and to the intersheet spacing, respectively (Fig. 4). Under chosen conditions, stefin A diffraction pattern differs from the one of stefin B in the sharpness of the concentric rings, with the one at 4.7 Å being sharper than in stefin B.

AFM

As shown in Figure 5, the amyloid fibrils of stefin A and stefin B are quite similar. They are both of indefinite lengths, varied from 50 nm up to several microns. However, for stefin A [Fig. 5(A)] we have observed two

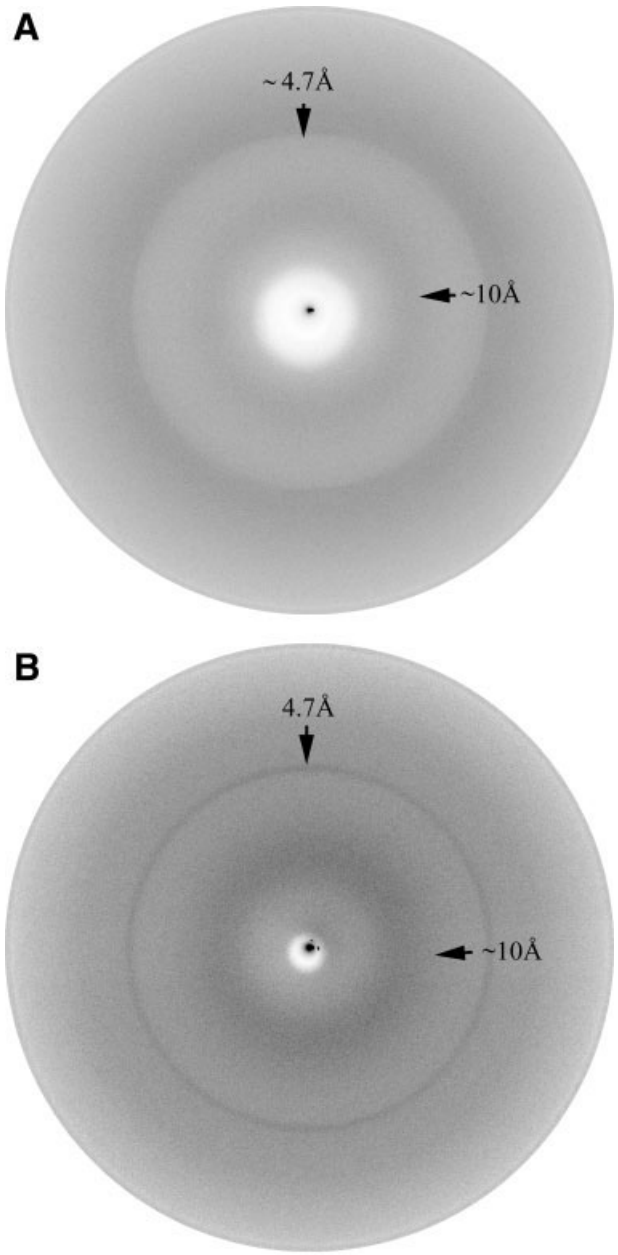

Fig. 4. **A:** X-ray fiber diffraction pattern of partially aligned stefin B, pH 4.8, 10% TFE. Fibrils grew 4 months in a 2-T magnet. **B:** X-ray fiber diffraction pattern of partially aligned stefin A with added seed, pH 2.48. Fibrils grew 4 months in a 2-T magnet.

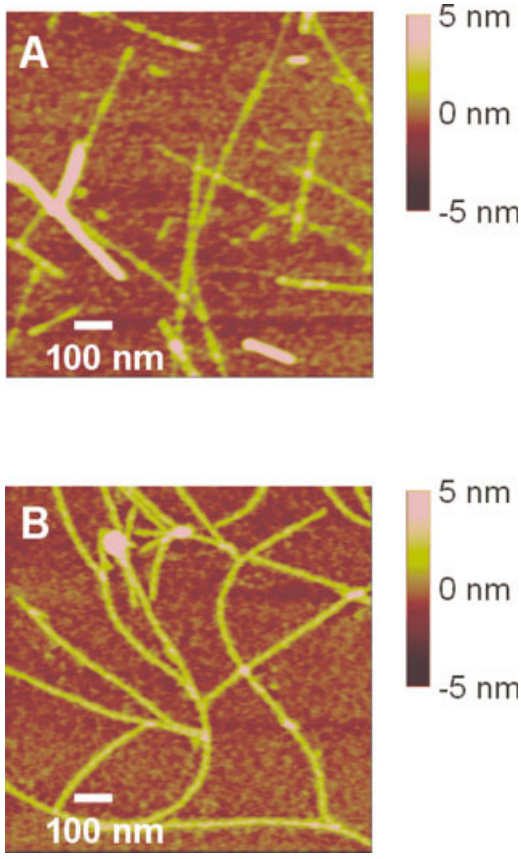

Fig. 5. AFM image of amyloid fibrils of stefins. Stefin A (**A**) and stefin B (**B**) adsorbed on the mica surface. Images were obtained in contact mode, and they represent height variation. Stefin A forms two types of fibrils according to the heights. The height of thinner fibrils is ~2.8 nm, and the height of thicker ones is ~5.6 nm. The height of fibrils of stefin B is constant at ~3.4 nm. The length of both fibrils varies from 50 nm up to several microns, and all the fibrils show periodicity in height with a period of ~26 nm.

types of fibrils according to their height, whereas in stefin B [Fig. 5(B)], all fibrils have the same height. Thinner fibrils of stefin A have an average height of 2.8 ± 0.4nm and show periodicity of 25 ± 2 nm with amplitudes of 0.9 ± 0.3 nm. Thicker fibrils of stefin A have an average height of 5.6 ± 0.5 nm, and they show similar periodicity as the thinner fibrils (i.e., 26 ± 2 nm with the amplitude 0.8 ± 0.3 nm. On the other hand, we have measured and already reported[28] that fibrils formed by stefin B had the same height of 3.4 ± 0.3 nm, and they showed periodicity of 27 ± 2nm.

TEM

TEM data of stefin B and its site-specific mutant amyloid fibrils have been collected before.[28,29] Two kinds of fibrils have been observed: the ones with a width of 6–7 nm (filaments) and the ones with a width of 12–14 nm (fibrils). Stefin A filaments/fibrils have also been measured by TEM (E. Žerovnik, M. Pompe-Novak, M. Tušek, and M. Ravnikar, unpublished data). The width of stefin A fibrils varied in different preparations but was always between 7 and 15 nm, in accordance with TEM data on stefin B.[28]

DISCUSSION

Amyloid Fibril Formation—A Universal Process?

The reflections at ~4.7 Å on the meridian and 10 Å on the equator are characteristic for amyloid fiber diffraction. The repeat of ~4.7 Å along the fiber axis, which corresponds to the spacing of β-strands and the ~10 Å distance, corresponding to the spacing between the β-sheets, are observed with stefin A and B fibrils [Figs. 4(A) and (B)]. The concentric rings apparently differ in sharpness, which could be due to differences in structural arrangement of the β-sheets.

We have used AFM [Figs. 5(A) and (B)] to determine lengths of the fibrils and their height profiles, whereas the estimated widths are too big due to the finite size of the tip, which causes apparent broadening of the fibrils. Measurements of the width by TEM are more reliable (not shown). By AFM, we have also determined periodicity and amplitudes of the height variations, with both fibrils showing the same periodic repeat of 25–27 nm. Similar periodicity of 25 nm along the fibril axis was observed by other authors for some other protein amyloid fibrils.[15]

Thus, our studies are in agreement with the hypothesis that the ability to form amyoid fibrils is generic to proteins.[32,38,39] The two homologous proteins, human stefins A and B, despite marked differences in stability and folding/unfolding rates, do form amyloid fibrils of the same overall structure. X-ray diffraction and AFM data are in agreement with amyloid fibrils of other proteins.

What Influences the Amyloid Fibril Growth?

Choosing the solvent

TFE was used with other proteins to induce amyloid fibril formation.[38,40] This organic solvent[41] reduces dielectric constant, making ionic interactions stronger. It is well known that hydrogen bonding is promoted by TFE, leading into an all α-helical state.[42] Titration by TFE of both stefins has been done,[23] and they both transformed into the all α-helical denatured state. To promote amyloid fibril formation by stefin B only predenaturational concentrations of TFE were found effective.[28] In this study, we have shown that TFE at predenaturational concentrations accelerates the fibril growth of both stefins A and B. That seeding accelerates fibrils' growth has been confirmed with both stefins, too.

Influence of a strong magnetic field

We also have shown that growing amyloid fibrils in a 2.3-T magnet accelerates their growth, which has not been reported before. There are reports in the literature[7,9,10] that strong magnetic field can be used to orient and align the fibers. Usually this was successful with shorter peptides, as shown for A-beta.[9] The magnetic field accelerated fibril growth of both stefins, but only with the samples where seeds were present. This finding perhaps could be interpreted as if the magnetic field exhibited its effect on the phase of growth and not the phase of nucleation.

Role of the initial conformation

The less stable stefin B undergoes fibrillation at milder conditions than stefin A. The process of fibrillation can start from either a native-like intermediate (pH < 5) or from a structured molten globule state (pH 3, 0.26 M sulfate). Even though the rate of fibril growth is higher and the lag phase shorter when starting from the state at pH 3, the regularity of the fibrils obtained is lower.[30]

Role of domain swapping

To form amyloid fibrils from the more stable stefin A, preheating is a necessary step. By knowing that this protein forms domain-swapped dimers at 84–92°C (predenaturational temperatures),[19] one can speculate that these form basic building blocks in the amyloid fibrils of cystatins.[20,31] An additional step required is reducing pH to 2.4, which is the midpoint of stefin A acid denaturation. Therefore, the domain-swapped dimers have to unfold, at least partially. Just heating the protein at neutral pH or reducing pH does not lead to amyloid fibrils. It is of note that monellin, a structural homologue of stefins from a plant source, had to be heated before being dissolved at a low pH, to form amyloid fibrils.[43]

What Makes Some Proteins More Amyloidogenic Than the Others?

General observations

A common observation is that discordance between the secondary structure prediction and the real secondary structure is predictive for amyloidogenic proteins.[44] The rationale for why some proteins are more amyloidogenic than the others is not clear. Repulsive ionic interactions may prevent fibril formation, consistent with the observations that neutralization of aspartate or glutamate residues leads to fibril formation. Native-state stability and slow rate of unfolding make fibrillation less likely.[44]

Contribution of salt bridges in stefins

In Figure 1, the 3D structures of stefin A and B monomers [Figs. 1(a) and (c)] and of stefin A domain-swapped dimer [Fig. 1(b)] are presented, whereas the domain-swapped dimer of stefin B has been modeled [Fig. 1(d)]. The core cystatin fold is retained in the dimers. Each cystatin-fold unit in the domain-swapped dimer is constituted by strand 1, the α-helix and strand 2 from one monomer, and strands 3–5 from the other monomer.[20,21] The interchangeable tandem of α-helix and strand 2 of stefin A monomer and dimer are attached via three salt bridges to the β-surface (strands 3–5), whereas in stefin B, there are none. This finding suggests that the interchangeable α-helix-strand 2 tandem of stefin B are more flexible than that of stefin A. An easier detachment of the α-helix from the β-sheet could explain, why stefin B forms folding intermediates[25] and amyloid fibrils[28,30] already at very mild acid conditions, in contrast to stefin A.

Other differences in structure and sequence of stefins

For amyloidogenesis, other factors than salt bridges may be important. We have looked for the so-called "dangling" hydrogen bonds and "inward-pointing" charged residues in both stefins.[44] We could not find any of those either in stefin A or in stefin B. There is no major difference in the overall number of hydrogen bonds and salt bridges in both proteins.

Secondary structure prediction was made by applying several methods (Table I). By various software programs of Jpred,[45] the α-helical part is predicted as either helical (extending to residue 47 or 42 in stefin A and B, respectively) or as extended (β-sheet). Similar discordance was found by using hierarchical neural network,[46] which predicts helix from 14 to 32, or by SOPMA,[47] which predicts an α-helix from residue 14 to 46, for both proteins. The discordance between real secondary structure (α-helix

TABLE I. Secondary Structure Prediction for the α-Helical Part of Both Stefins[†]

α-Helix	Stefin B	Stefin A
Real structure/X-ray	13–32	13–32
SSP program	Prediction	Prediction
SOPMA[a]	14–46	14–46
HNN[b]	14–32	15–22 & 37–41
Jalign[c]	35–41	15–20 & 36–46
Jfreq[c]	13–42	13–27 & 33–42
Jpred[c]	13–30	14–30

[†]The whole sequence was analyzed by using the secondary structure prediction (SSP) programs available on the net.
[a]Geourjon C, Deleage G. 1995: SOPMA.[47]
[b]Combet et al., 2000.[46]
[c]Cuff et al., 1998.[45]

from 13 to 32) and overprediction to residue 46 indicates the tendency of these proteins to form amyloid fibrils. Perhaps they both first have to transform into a non-native α-helical intermediate, such as observed with Aβ.[48] This is quite consistent with observations made with stefin B, where an α-helical folding intermediate has been observed in folding[22,23] and on the route to amyloid fibril formation.[30]

CONCLUSION

Many features of the process of amyloid fibril formation observed for the two human stefins are in common with other proteins: globular or natively unfolded, confirming its generic nature. Difference in the propensity to undergo fibrillation of the two homologues can partially be explained by the higher stability of stefin A and its low rate of unfolding.[49] We suggest that a major part of the difference in stability between the two human stefins stems from the arrangement of salt bridges, which could prevent detachment of the secondary structure elements (α-helix from β-sheet) both in stefin A monomer and domain-swapped dimer.

ACKNOWLEDGMENTS

We thank Dr. Igor Serša (JSI, Ljubljana) for kindly giving us an opportunity to grow fibrils in a 2.35-T magnet of the 100 MHz Brucker Biospec System NMR machine. We also thank Prof. Maja Ravnikar (NIB, Ljubljana) for letting us discuss unpublished TEM data.

REFERENCES

1. Cohen AS. General introduction and brief history of the amyloid fibril. In: Marrink J, Van Rijswijk MH, editors. Amyloidosis. Dordrecht: Nijhoff; 1986. p 3–19.
2. Sipe JD, Cohen AS. Review: history of the amyloid fibril. J Struct Biol 2000;130:88–98.
3. Goedert M, Spillantini MG, Davies SW. Filamentous nerve cell inclusions in neurodegenerative diseases. Curr Opin Neurobiol 1998;8:619–632.
4. Cohen FE. Prions, peptides and protein misfolding. Mol Med Today 2000;6:292–293.
5. Soto C. Protein misfolding and disease; protein refolding and therapy (review). FEBS Lett 2001;498:204–207.
6. Blake C, Serpell L. Synchrotron X-ray studies suggest that the core of the transthyretin amyloid fibril is a continuous β-sheet helix. Structure 1996;4:989–998.
7. Sunde M, Serpell LC, Bartlam M, Fraser PE, Pepys MB, Blake CCF. Common core structure of amyloid fibrils by ;Synchrotron X-ray diffraction J Mol Biol 1997;273:729–739.
8. Kirschner D, Elliott-Brant R, Szumowski KE, Gonnerman WA, Kindy, MS, Sipe JD, Cathcart ES. In vitro amyloid fibril formation by synthetic peptides corresponding to the amino terminus of apoSAA isoforms from amyloid-susceptible and amyloid-resistant mice. J Struct Biol 1998;124:88–98.
9. Malinchik SB, Inouye H, Szumowski KE, Kirschner DA. Structural analysis of Alzheimer's β(1-40) amyloid: protofilament: assembly of tubular fibrils. Biophys J 1998;74:537–545.
10. Serpell LC, Fraser PE, Sunde M. X-ray fiber diffraction of amyloid fibrils. Methods Enzymol 1999;309:526–537.
11. Stine WB, Snyder SW, Ladror US, Wade WS, Miller MF, Perun TJ, Holzman TF, Krafft GA. The nanometer-scale structure of amyloid-beta visualized by atomic force microscopy. J Protein Chem 1996;15:193–203.
12. Ding TT, Harper JD. Analysis of amyloid-beta assemblies using tapping mode atomic force microscopy under ambient conditions. Methods Enzymol 1999;309:510–525.
13. Goldsbury CS, Cooper GJ, Goldie KN, Muller SA, Saafi EL, Gruijters WT, Misur MP, Engel A, Aebi U, Kistler J. Polymorphic fibrillar assembly of human amylin. J Struct Biol 1997;119:17–27.
14. Ionescu-Zanetti C, Khurana R, Gillespie JR, Petrick JS, Trabachino LC, Minert LJ, Carter SA, Fink AL. Monitoring the assembly of Ig light-chain amyloid fibrils by atomic force microscopy. Proc Natl Acad Sci USA 1999;96:13175–13179.
15. Goldsbury C, Kistler J, Aebi U, Arvine T, Cooper GS. Watching amyloid fibrils grow by time-lapse atomic force microscopy. J Mol Biol 1999;285:33–39.
16. Stubbs MT, Laber B, Bode W, Huber R, Jerala R, Lenarčič B, Turk V. The refined 2.4 Å X-ray structure of recombinant human stefin B in complex with the cysteine proteinase papain: a novel type of proteinase inhibitor interaction. EMBO J 1990;9:1939–1947.
17. Jenko S, Dolenc I, Gunčar G, Doberšek A, Podobnik M, Turk D. Crystal structure of stefin A in complex with cathepsin H: N-terminal residues of inhibitors can adapt to the active sites of endo- and exopeptidases. J Mol Biol 2003;326:875–885.
18. Martin JR, Craven CJ, Jerala R, Kroon-Žitko L, Žerovnik E, Turk V, Waltho JP. The three-dimensional solution structure of human stefin A. J Mol Biol 1995;246:331– 343.
19. Jerala R, Žerovnik E. Accessing the global minimum conformation of stefin A dimer by annealing under partially denaturing conditions. J Mol Biol 1999;291:1079–1089.
20. Staniforth RA, Giannini S, Higgins LD, Conroy MJ, Hounslow AM, Jerala R, Craven CJ, Waltho JP. Three-dimensional domain swapping in the folded and molten-globule states of cystatins, an amyloid-forming structural superfamily. EMBO J 2001;20:4774–81.
21. Janowski R, Kozak M, Jankowska E, Grzonka Z, Grubb A, Abrahamson M, Jaskolski M. Human cystatin C, an amyloidogenic protein, dimerizes through three-dimensional domain swapping. Nat Struct Biol 2001;8:316–320.
22. Žerovnik E, Virden R, Jerala R, Turk V, Waltho JP. On the mechanism of human stefin B folding. I. Comparison to homologous stefin A. Influence of pH and trifluoroethanol on the fast and slow folding phases. Proteins 1998;32:296–303.
23. Žerovnik E, Virden R, Jerala R, Kroon-Žitko L, Turk V, Waltho JP. Differences in the effects of TFE on the folding pathways of human stefins A and B. Proteins 1999;36:205–216.
24. Žerovnik E, Jerala R, Kroon-Žitko L, Pain RH, Turk V. Intermediates in denaturation of a small globular protein, recombinant human stefin B. J Biol Chem 1992a;267:9041–9046.
25. Žerovnik E, Jerala R, Kroon-Žitko L, Turk V, Lohner K. Characterization of the equilibrium intermediates in acid denaturation of human stefin B. Eur J Biochem 1997;245:364–372.
26. Žerovnik E, Lohner K, Jerala R, Laggner P, Turk V. Calorimetric measurements of thermal denaturation of stefins A and B; comparison to predicted thermodynamics of stefin B unfolding. Eur J Biochem 1992b;210:217–221.
27. Hamada D, Segawa S, Goto Y. Non-native alpha-helical intermediate in the refolding of beta-lactoglobulin, a predominantly beta-sheet protein. Nat Struct Biol 1996;3:868–873.
28. Žerovnik E, Pompe-Novak M, Škarabot M, Ravnikar M, Muševič I, Turk V. Human stefin B readily forms amyloid fibrils in vitro. Biochim Biophys Acta 2002a;1594:1–5.
29. Žerovnik E, Zavašnik-Bergant V, Kopitar-Jerala N, Pompe-Novak M, Škarabot M, Goldie K, Ravnikar M, Muševič I, Turk V. Amyloid fibril formation by human stefin B in vitro: ;Immunogold

labelling and comparison to stefin A. Biol Chem 2002b;383:859–863.
30. Žerovnik E, Turk V, Waltho JP. Amyloid fibril formation by human stefin B: influence of the initial pH-induced intermediate state. Biochem Soc Trans 2002c;30:543–547.
31. Žerovnik E. Amyloid-fibril formation: proposed mechanisms and relevance to conformational disease. Eur J Biochem 2002;69:3362–3371.
32. Dobson CM. Getting out of shape. Nature 2002;418:729–730.
33. Bucciantini M, Giannoni E, Chiti F, Baroni F, Formigli L, Zurdo J, Taddei N, Ramponi G, Dobson CM, Stefani M. Inherent toxicity of aggregates implies a common mechanism for protein misfolding diseases. Nature 2002;416:507–511.
34. Kenig M, Jerala R, Kroon-Žitko L, Žerovnik E, Turk V. Major differences in stability and dimerization properties of two chimeric mutants of human stefins. Proteins 2001;42:512–522.
35. Jerala R, Trstenjak M, Lenarčič B, Turk V. Cloning a synthetic gene for human stefin B and its expression in E. coli. FEBS Lett 1988;239:41–44.
36. Turk D. Weiterentwicklung eines Programms für Molekülgraphik und Elektrondichte-manipulation und seine Anwendung auf verschiedene Protein-strukturaufklärungen. PhD thesis, Technische Universität, München., 1992.
37. Levine H. Quantification of β-sheet amyloid fibril structures with thioflavin T. Methods Enzymol 1999;309:274–284.
38. Guijarro JI, Sunde M, Jones JA, Campbell ID, Dobson CM. Amyloid fibril formation by an SH3 domain. Proc Natl Acad Sci USA 1998;95:4224–4228.
39. Dobson CM. Protein misfolding, evolution and disease. Trends Biochem Sci 1999;24:329–332.
40. Chiti F, Webster P, Taddei N, Clark A, Stefani M, Ramponi G, Dobson CM. Designing conditions for in vitro formation of amyloid protofilaments and fibrils. Proc Natl Acad Sci USA 1999;96:3590–3594.
41. Buck M. Trifluoroethanol cosolvents come of age. Recent studies with peptides and proteins. Q Rev Biophys 1998;31:297–355.
42. Hamada D, Goto Y. The equilibrium intermediate of β-lactoglobulin with non-native α-helical structure. J Mol Biol 1997;269:479–487.
43. Konno T, Murata K, Nagayama K. Amyloid-like aggregates of a plant protein: a case of a sweet-tasting protein, monellin. FEBS Lett 1999;454:122–126.
44. Thirumalai D, Klimov DK, Dima RI. Emerging ideas on the molecular basis of protein and peptide aggregation. Curr Opin Struct Biol 2003;13:146–159.
45. Cuff JA, Clamp ME, Siddiqui AS, Finlay M, Barton GJ. Jpred: a consensus secondary structure prediction server. Bioinformatics 1998;14:892–893.
46. Combet C, Blanchet C, Geourjon C, Deleage G. NPS@: network protein sequence analysis. Trends Biochem Sci 2000;25:147–150.
47. Geourjon C, Deleage G. SOPMA: Significant improvement in protein secondary structure prediction by consensus prediction from multiple alignments. Cabios 1995;11:681–684.
48. Kirkitadze MD, Condron MM, Teplow DB. Identification and characterization of key kinetic intermediates in amyloid beta-protein fibrillogenesis. J Mol Biol 2001;312:1103–1119.
49. Kenig M. Stability and rate of folding of chimeric and some site-specific mutants of human stefins. PhD thesis, University of Ljubljana, Slovenia, 2002.
50. Merritt EA, Bacon DJ. Raster3D: photorealistic molecular graphics. Methods Enzymol 1997;277:505–524.